

Focused-ion-beam platinum nanopatterning for GaN nanowires: Ohmic contacts and patterned growth

C. Y. Nam, J. Y. Kim, and J. E. Fischer^{a)}

Department of Materials Science and Engineering, University of Pennsylvania, 3231 Walnut Street, Philadelphia, Pennsylvania 19104-6272

(Received 21 January 2005; accepted 25 March 2005; published online 5 May 2005)

Nanopatterned Pt by Ga⁺ focused ion beam (FIB) decomposition of an organometallic precursor forms low resistance ohmic contacts on 40–70 nm diameter GaN nanowires (NWs) grown by thermal reaction of Ga₂O₃ and NH₃. With no intentional doping, the wires are presumed to be *n* type. Thus, the linear *I-V* behavior is surprising since evaporated Pt usually forms Schottky barriers on *n* GaN. Ohmic behavior was not obtained for 130–140 diameter wires, even with thicker Pt contacts. A second application of FIB Pt nanopatterning was demonstrated by position-selective growth of GaN NWs on Pt catalyst dots. NW locations and density are defined by the position, size, and thickness of the Pt deposit. Combining these techniques provides a versatile platform for nanostructure research and development. © 2005 American Institute of Physics. [DOI: 10.1063/1.1925775]

Achieving reliable low resistance ohmic contacts to GaN is not trivial. High contact resistance often degrades the performance of GaN-based devices.¹ Low resistance ohmic contacts to *n*-type GaN are generally obtained by Ti deposition and conventional lithography. Similar metals and methods have been applied to GaN nanowires (NWs),^{2,3} but these require a tedious sequence of locating NWs on a substrate by atomic force microscopy, defining a contact pattern with electron-beam (e-beam) lithography, metal deposition, and removal of e-beam resist. In addition, achieving robust ohmic contacts requires work function tuning and deposition of an adhesion layer to insure mechanical stability.

Attracted by its convenience and versatility, several groups reported the use of direct Pt deposition by focused ion beam (FIB) to make metal contacts on Bi and Ag NWs (Refs. 4 and 5) and carbon nanotubes.⁵ This is done by locally decomposing a fine jet of organometallic vapor with the highly focused and spatially controlled Ga⁺ ion beam (I-beam).⁵ Since most FIB systems are also equipped with high-resolution scanning electron microscopy (SEM), the combination provides unique capabilities of fast and precise metal contact patterning. Here, we demonstrate direct FIB nanopatterning of low resistance ohmic Pt contacts on *n*-type GaN NWs grown by Ga₂O₃–NH₃ reaction without intentional doping. It is surprising for FIB patterned Pt to form low resistance ohmic contacts on *n*-type GaN since Pt generally forms a Schottky barrier on *n*-type GaN.⁶ In the second part of this letter, we exploit the same spatial selectivity to create patterned Pt nanocatalysts, which constrain GaN NW nucleation to these small selected regions.

The details of GaN NW synthesis are described in a previous report.⁷ We used sputter-deposited Au/Pd catalyst layers on Si substrates. Two different layer thicknesses yielded two different NW diameters, i.e., 40–70 nm and 130–140 nm, with which we could study the effect of NW diameter on current-voltage (*I-V*) characteristics. NWs were then transferred to 200 nm SiO_x on Si chips with Cr/Au

(10 μm/50 μm) contact pads predeposited by e-beam lithography and thermal evaporation. These were loaded into an FEI Strata DB235 FIB system⁸ with SEM capability. NWs were quickly located and selected with SEM. FIB-Pt contacts were directly written to bridge the NW to the Cr/Au pads. We used 30 kV Ga⁺ at 10–30 pA to decompose trimethylcyclopentadienyl-platinum [(CH₃)₃CH₃C₅H₄Pt] into a predetermined bridging lead. The dwell time was 0.2 μs per pixel with ~50% overlap. Figure 1(a) shows a representative SEM image of a FIB-Pt patterned two-probe device. The nominal Pt thickness was 100–150 nm, and the width and length were 250–700 nm and 5–7 μm respectively. In general, I-beam deposition conditions must be carefully chosen to avoid significant damage or complete destruction of the sample by massive Ga⁺ ions.⁵ We found no evidence for such damage, but minor sputtering around the contact area was observed [Fig. 1(b) inset]. This might in fact improve contact properties by removing surface oxide.⁴ We examined spreading of deposited Pt beyond the desired areas using I-beam images, which are in effect Z-contrast images and thus very sensitive to the heavy Pt. As shown in Fig. 1(b), no device shorting was seen, so the Pt spillover is probably thin. Nonetheless, to prevent possible shorting from Pt spreading, we kept the device length 5 μm or greater, and the Pt deposition time around the NW area less than 30 s. This conservative design eliminates the possibility of shorting as corroborated by the *I-V* results described next.

Figure 2(a) shows representative *I-V* curves of the FIB patterned NW devices from two batches of NWs. The smaller diameter NW device displays a linear behavior while the larger one shows nonlinear *I-V* characteristics. Resistivities (neglecting contact resistance) were as low as 0.04 Ω cm for the smaller diameter and 1.3 Ω cm for the larger one (from the zero-bias slopes). We studied three devices from each batch, and the diameter dependence of *I-V* characteristics and the resistivity value were consistent throughout. Neither batch exhibited gate response in the range ±9 V. To study the effect of Pt thickness on contact properties, 250 nm Pt was patterned on the larger diameter NWs, but as shown in Fig. 2(a), the *I-V* characteristics still displayed the same

^{a)} Author to whom correspondence should be addressed; electronic mail: fischer@seas.upenn.edu

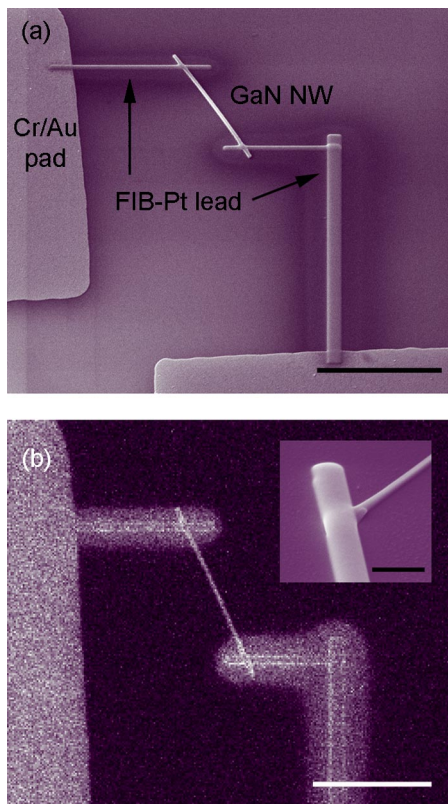


FIG. 1. (Color online) (a) SEM image of two-probe GaN NW device with contacts patterned by FIB-Pt deposition. The scale bar is 5 μm . (b) I-beam image (Z-contrast) revealing Pt spreading around the FIB-Pt leads (white scale bar: 5 μm). Inset shows details of FIB Pt-contact: The NW is 63 nm wide, and the width of the contact line is 250 nm (scale bar: 500 nm).

nonlinear behavior with a similar resistivity to the device with 150 nm Pt, thus suggesting the relative thickness of Pt is *per se* not related with the origin of nonlinear I - V behavior.

To further rule out leakage currents from Pt spillover, we fabricated two-probe devices from the smaller diameter NWs by conventional e-beam lithography and 100 nm thick sputtered Pt contacts [Fig. 2(b) inset]. These devices showed nonlinear I - V with a resistivity as high as $\sim 1000 \Omega \text{ cm}$ [Fig. 2(b)]. Again, no gate response was observed, confirming that its absence is inherent to NWs grown by our technique. The low two-probe resistivity of the smaller NWs, measured from FIB-Pt contacted devices, argues directly against shorting by Pt. Assuming a Pt coating in parallel with the GaN NW, the measured resistance R_{measured} is given by $1/R_{\text{measured}} = 1/R_{\text{NW}} + 1/R_{\text{Pt}}$, where R_{NW} and R_{Pt} are resistances of NW and Pt, respectively. In order for R_{Pt} to be significant, say $R_{\text{NW}} \approx R_{\text{Pt}}$, and assuming the resistivity of bulk Pt at 300 K, the effective Pt thickness should be of order pm, or ~ 0.01 monolayer coverage, which would be well below a percolation threshold.

The absence of gate response is common to GaN NW with FIB- and sputter-deposited Pt contacts, and must therefore be specific to our growth method. A likely explanation is inadvertent heavy n -type autodoping by O or Si released during growth,^{9,10} by the reduction of Ga_2O_3 by NH_3 or from the quartz liner tube, respectively. Electron energy loss spectra measured on each batch qualitatively confirmed the presence of O and the absence of typical p -type impurities, e.g., Mg. Thus, we can safely assume that our GaN NW is n type.

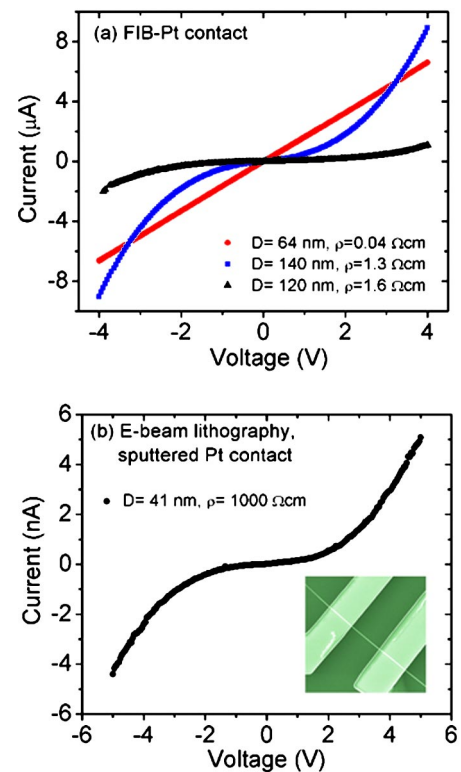


FIG. 2. (Color online) (a) Two-probe I - V data from FIB-Pt contacted GaN NW. D and ρ denote diameter of NW and resistivity calculated from zero-bias resistance. Nominal Pt thickness 150 (250) nm for wire diameters 64, 140 (120) nm. The smallest diameter NW shows linear I - V behavior in the bias window ± 4 V, while the larger diameter NWs display nonlinear I - V . The 120 nm NW is \sim four times longer than the other two, thus the smaller current at all V. (b) Nonlinear I - V behavior of another small-diameter NW with 100 nm sputtered Pt contacts defined by e-beam lithography (inset). The resistivity is $\sim 20,000$ times greater than a wire from the same batch with FIB-Pt.

Since Pt is normally used for Schottky barrier contacts on n -type GaN,⁶ we were surprised to find low resistance and linear I - V from our FIB-Pt contacts. This is under further investigation, but we suspect that Ga^+ I-beam irradiation around the contact area plays a role. Dhara *et al.*¹¹ reported that 50 kV FIB- Ga^+ implantation induces amorphization of GaN NW. The inset to Fig. 1(b) suggests the possibility of partial amorphization around the contact area by our 30 kV Ga^+ I-beam. The resistivity of amorphous GaN can be less than $\sim 180 \Omega \text{ cm}$ due to the formation of Ga-Ga homopolar bonds when a Ga/N ratio > 1 .^{12,13} This would apply to our NWs due to Ga implantation into the I-beam damaged region. If the amorphous GaN were sufficiently Ga rich, it could provide an excellent work function match (4.2 eV for Ga metal) to the 4.1 eV electron affinity of n -type GaN. In a recent report, Pt NW fabricated by FIB-Pt deposition was shown to actually consist of Pt crystallites and the amorphous matrix of Ga and C.¹⁴

Finally, we present a second application of FIB Pt nanopatterning, namely catalyzed GaN NW growth. The ability to organize nanostructures into functional hierarchical patterns is an important and difficult technological challenge. A successful example is the postgrowth patterning of NW by a fluidic assembly.¹⁵ In some cases, one could envision gains in efficiency and/or performance if the location and/or crystallographic orientation of NW growth could be directly controlled. Positional control of GaN NW growth has been

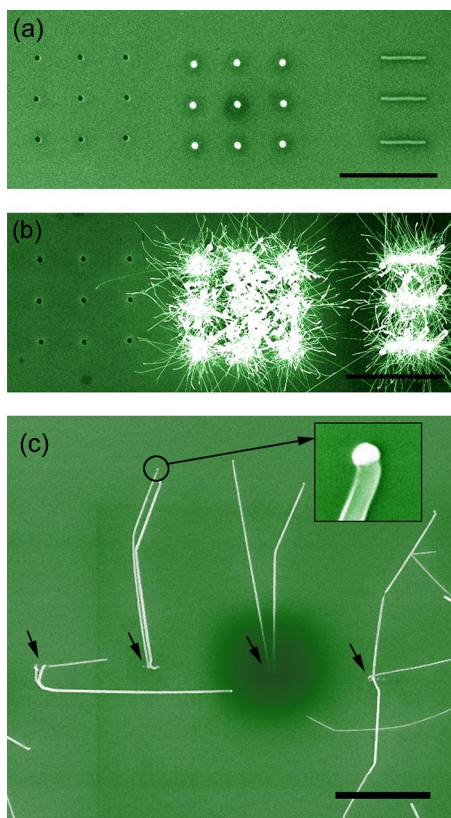


FIG. 3. (Color online) (a) FIB patterned template before GaN growth. From left to right, FIB milled holes, Pt dots and lines. Depth of hole is 150 nm, and thickness of dots and lines are 250 nm. Separation between features is 5 μm (scale bar: 10 μm). (b) The template in (a) after NW growth. NWs preferentially grew at the patterned Pt dots and lines, while milled holes did not nucleate NW growth (scale bar: 10 μm). (c) Individual GaN NWs grown at FIB-Pt dots (scale bar: 5 μm). Diameters of dots reduced to 250 nm with same 5 μm spacing. Inset shows a magnified image of spherical particle on the tip of grown NW. The diameters of NW and the particle are ~ 60 nm and ~ 65 nm, respectively.

achieved by a dip-pen method.¹⁶ Patterned growth of other nanostructures utilizing FIB was demonstrated using Ga⁺ ion-implanted substrates or Ga⁺ I-beam milled masks.^{17,18} Another alternative is positional control of NW growth by FIB-Pt patterning of nanoscale catalyst islands, or dots.

Figure 3(a) shows FIB milled holes, Pt dots, and Pt lines patterned on SiO_x/Si (200 nm SiO_x) in preparation for catalytic area-selective GaN NW growth. The nominal diameters of holes and dots are 1 μm , and the lines are 1 μm wide and 5 μm long. The holes are 150 nm deep, and the Pt thickness was 250 nm throughout. Using this template, GaN NW growth was carried out by Ga₂O₃-NH₃ thermal reaction at the substrate temperature of ~ 900 °C. As shown in Fig. 3(b), NW nucleation and growth occurred only at the patterned Pt dots or lines. Wires grew in random directions and the nucleation density was too high to observe individual NW. Ga⁺ I-beam milling alone did not nucleate NW growth, confirming that Pt is acting as a catalyst.

To achieve well-separated NW's with one end at a defined location, we reduced the nucleation density by reducing the size of the dots and decreasing the growth time. Figure 3(c) displays individual NWs grown out of 250 nm diameter dots with the same 5 μm grid spacing and Pt thickness as before. Arrows indicate the original dot positions, which match the roots of grown NWs. The spherical particles on

the NW tips [Fig. 3(c) inset] are presumably Pt (to be confirmed), suggesting a vapor-liquid-solid root growth mechanism. For this to be true, the 1789 °C bulk melting point of Pt would have to be depressed to the 900 °C substrate temperature during growth. This can be attributed to a combination of Pt particle size effect¹⁹ and Ga alloying.

In summary, we have demonstrated two important applications of FIB-Pt nanopatterning. We achieved low resistance ohmic Pt contacts on *n*-type GaN NW using FIB-Pt deposition. The technique significantly reduces the nanodevice fabrication time and insures low resistance ohmic contacts, which is essential for electrical characterization of NWs. The formation of ohmic contact is surprising since Pt normally forms Schottky barrier on *n*-type GaN. The nature of the contact formation needs further investigation. We also demonstrated positional control of GaN NW growth by FIB patterning of Pt catalyst dots. The nucleation density can be controlled by changing the size of dots, and the small dots initiated the growth of individual NWs in more controlled manner. Both techniques can be applied to other nanostructure systems. An obvious extension would be to find a way to integrate patterned growth and device fabrication into a single process.

The authors are grateful to D. Tham and K.H. Byon for helping with TEM and e-beam patterning respectively. This work was supported by USDOE Grant No. DE-FG02-98ER45701 (for one of the authors—C.Y.N.) and NSF/NIRT Grant No. DMR03-04178 (for another author—J.Y.K.). The authors also acknowledge the use of shared facilities supported by NSF/MRSEC: DMR02-03378.

¹M. E. Lin, Z. Ma, F. Y. Huang, Z. F. Fan, L. H. Allen, and H. Morkoç, Appl. Phys. Lett. **64**, 1003 (1994).

²Y. Huang, X. Duan, Y. Cui, and C. M. Lieber, Nano Lett. **2**, 101 (2002).

³J.-R. Kim, H. Oh, H. So, J.-J. Kim, J. Kim, C. J. Lee, and S. C. Lyu, Nanotechnology **13**, 701 (2002).

⁴S. B. Cronin, Y.-M. Lin, O. Rabin, M. R. Black, J. Y. Ying, M. S. Dresselhaus, P. L. Gai, J.-P. Minet, and J.-P. Issi, Nanotechnology **13**, 653 (2002).

⁵V. Gopal, V. R. Radmilovic, C. Daraio, S. Jin, P. Yang, and E. A. Stach, Nano Lett. **4**, 2059 (2004).

⁶L. Wang, M. I. Nathan, T.-H. Lim, M. A. Khan, and Q. Chen, Appl. Phys. Lett. **68**, 1267 (1996).

⁷C. Y. Nam, D. Tham, and J. E. Fischer, Appl. Phys. Lett. **85**, 5676 (2004).

⁸<http://www.seas.upenn.edu/nanotechfacility/fib/index.html>

⁹W. Götz, N. M. Johnson, C. Chen, H. Liu, C. Kuo, and W. Imler, Appl. Phys. Lett. **68**, 3144 (1996).

¹⁰C. G. Van de Walle and J. Neugebauer, J. Appl. Phys. **95**, 3851 (2004).

¹¹S. Dhara, A. Datta, C. T. Wu, Z. H. Lan, K. H. Chen, Y. L. Wang, L. C. Chen, C. W. Hsu, H. M. Lin, and C. C. Chen, Appl. Phys. Lett. **82**, 451 (2003).

¹²A. Koo, U. D. Lanke, B. J. Ruck, S. A. Brown, R. Reeves, I. Liem, A. Bittar, and H. J. Trodahl, Mater. Res. Soc. Symp. Proc. **693**, I10.10.1. (2002).

¹³U. D. Lanke, A. Koo, S. Granville, J. Trodahl, A. Markwitz, J. Kennedy, and A. Bittar, Mod. Phys. Lett. B **15**, 1355 (2001).

¹⁴L. Rotkina, J.-F. Lin, and J. P. Bird, Appl. Phys. Lett. **83**, 4426 (2003).

¹⁵Y. Huang, X. Duan, Q. Wei, and C. M. Lieber, Science **291**, 630 (2001).

¹⁶J. Y. Li, C. Lu, B. Maynor, S. Huang, and J. Liu, Chem. Mater. **16**, 1633 (2004).

¹⁷Y. T. Sun, E. R. Messmer, S. Lourduodoss, J. Ahopelto, S. Rennon, J. P. Reithmaier, and A. Forchel, Appl. Phys. Lett. **79**, 1885 (2001).

¹⁸S. W. Kim, T. Kotani, M. Ueda, S. Fujita, and S. Fujita, Appl. Phys. Lett. **83**, 3593 (2003).

¹⁹M. Zhang, M. Y. Efremov, F. Schiettekatte, E. A. Olson, A. T. Kwan, S. L. Lai, T. Wisleder, J. E. Greene, and L. H. Allen, Phys. Rev. B **62**, 10548 (2000).